Geoscience Frontiers 12 (2021) 101137

HOSTED BY

Contents lists available at ScienceDirect

Geoscience Frontiers

journal homepage: www.elsevier.com/locate/gsf

Ga isotopic fractionation in sulfides from the Yuhuang and Duanqiao hydrothermal fields on the Southwest Indian Ridge

Yuxu Zhang [a], Shili Liao [b], Chunhui Tao [b], Hanjie Wen [a,c,*], Haifeng Fan [a], Jing Wen [a,c], Weifang Yang [b], Wei Li [b]

[a] State Key Laboratory of Ore Deposit Geochemistry, Institute of Geochemistry, Chinese Academy of Sciences, Guiyang 550081, China
[b] Key Laboratory of Submarine Geosciences, Second Institute of Oceanography, Ministry of Natural Resources, Hangzhou 310012, China
[c] University of Chinese Academy of Sciences, Beijing 100049, China

ARTICLE INFO

Article history:
Received 8 August 2020
Received in revised form 28 October 2020
Accepted 16 December 2020
Available online 06 January 2021

Handling Editor: C. Spencer

Keywords:
Ga isotope
Hydrothermal sulfide
Yuhuang
Duanqiao
Southwest Indian Ridge

ABSTRACT

This study examines the Ga isotopic compositions of sulfides in the Yuhuang and Duanqiao hydrothermal fields on the Southwest Indian Ridge, mid-ocean ridge basalts (MORB), and calcareous sediments around the hydrothermal fields. The $\delta^{71/69}Ga_{NIST\text{-}994}$ values of the MORB samples vary little (+1.20‰ to +1.23‰, with an average of +1.22‰) and are consistent with the $\delta^{71/69}Ga_{NIST\text{-}994}$ values of two standard basalt samples (BCR-2 and BHVO-2), indicating that Ga isotopes may either not fractionate or fractionate only slightly under high-temperature geological processes; therefore, the $\delta^{71/69}Ga_{NIST\text{-}994}$ value of oceanic crust may be +1.22‰. The sediments (+1.28‰ to +1.47‰, with an average of +1.38‰) are rich in heavier Ga isotopes than the basalts, and the Ga present in the sediments may have originated from soluble Ga present in the seawater that was adsorbed by (Mn, Fe) oxides/hydroxides. The Ga contribution of basaltic debris to the sediments was almost negligible. Thus, we speculate that the $\delta^{71/69}Ga_{NIST\text{-}994}$ value of seawater in the study area fell within a range from +1.92‰ to +2.36‰. The $\delta^{71/69}Ga_{NIST\text{-}994}$ values of the sulfides in the Yuhuang hydrothermal field range from +0.99‰ to +1.57‰, with an average of +1.25‰, and the $\delta^{71/69}Ga_{NIST\text{-}994}$ values of the sulfides in the Duanqiao hydrothermal field range from +0.93‰ to +1.55‰, with an average of +1.19‰. The $\delta^{71/69}Ga_{NIST\text{-}994}$ ranges of the sulfides in the Yuhuang and Duanqiao hydrothermal fields are similar, with the Ga isotopic fractionation reaching 0.58‰ and 0.62‰, respectively. The average $\delta^{71/69}Ga_{NIST\text{-}994}$ values in the sulfides are close to those in the MORBs. This suggests that Ga within the sulfides in the Yuhuang and Duanqiao hydrothermal fields mainly originated from MORBs, with seawater and sediments making only small contributions. The Ga isotopic fractionation in the sulfides may be related to processes associated with the formation of sulfides, such as rapid precipitation or the admixture of different stages of sulfide. This study is of great significance for understanding the global distribution of Ga isotopes and the Ga cycle in submarine hydrothermal systems.

1. Introduction

Ga has two stable isotopes (^{69}Ga and ^{71}Ga) with natural elemental abundances of 60.1079% and 39.8921%, respectively (Meija et al. 2016; Kato et al., 2017). The Ga isotopic compositions of meteoritic samples and metal Ga were initially investigated in the early stages of geological research (Inghram et al., 1948; De Laeter 1972). However, the fractionation that occurs in the Ga isotopes of natural samples meant that mass spectrometers could not measure the variation in Ga isotopic compositions accurately, meaning that few studies investigating Ga isotopes have been carried out. The development of mass spectrometers with high accuracy and precision, such as the multi-collector inductivity coupled plasma mass spectrometer (MC-ICP-MS), and the improvements made in chemical separation and purification pretreatments (Yuan et al. 2016; Zhang et al. 2016; Kato et al., 2017) means that the accurate analysis of Ga isotopes is now possible. Previous studies have demonstrated distinct Ga isotopic fractionation of lunar and meteoritic samples, such as $\delta^{71/69}Ga_{NIST\text{-}994}$ values from +1.35‰ to +1.83‰ observed in lunar mare basalts, +0.83‰ to +1.28‰ seen in carbonaceous chondrites, and + 0.14‰ to +1.13‰ in ordinary chondrites (Kato et al., 2017; Kato and Moynier, 2017a,b). Different types of standard terrestrial geological samples have different Ga isotopic compositions (the maximum observed is 1.83‰) (Yuan et al. 2016; Zhang et al. 2016). Kato et al. (2017) found that the Ga isotopic compositions of terrestrial igneous samples are relatively homogeneous, and that the solid silicate Earth ($\delta^{71/69}Ga_{NIST\text{-}994}$ = +1.26‰ ± 0.06‰) is richer in lighter Ga isotopes than the Moon. The results of simulation experiments indicate that the process by which Ga is adsorbed onto mineral (calcite and goethite) surfaces leads to a distinct Ga isotopic fractionation, resulting in the solid phase being rich in lighter Ga

* Corresponding author at: State Key Laboratory of Ore Deposit Geochemistry, Institute of Geochemistry, Chinese Academy of Sciences, Guiyang 550081, China.
E-mail address: wenhanjie@vip.gyig.ac.cn (H. Wen).

https://doi.org/10.1016/j.gsf.2020.12.016

isotopes while the solution phase is rich in heavier Ga isotopes. The $\Delta^{71/69}Ga_{solid\text{-}solution}$ value of calcite can reach −1.27‰ and that of goethite can reach −0.89‰ (Yuan et al. 2018).

Ga is generally stored in bauxite deposits, Pb–Zn ore deposits, and coal deposits, with the Ga in coals mainly concentrated in boehmite and kaolinite (Liu 1982; Moskalyk 2003; Tu et al. 2003; Wang et al. 2011). Therefore, supergene weathering metallogenic systems and hydrothermal metallogenic systems are two important ore-forming processes that involve Ga. Hydrothermal Pb–Zn deposits demonstrate significant Ga storage; for example, the Ga concentration in sphalerite can reach 3000 μg/g (Fleischer 1955; Tu et al. 2003). However, the material source and enrichment mechanisms of Ga in hydrothermal Pb–Zn deposits are still unclear. The hydrothermal systems on the modern seafloor are optimum areas in which ancient hydrothermal metallogenic systems can be studied. Since the initial discovery of seafloor hot springs and high-temperature hydrothermal mineralization in 1977 (Corliss et al. 1979; Williams et al. 1979), more than 600 seafloor hydrothermal vents have been discovered (www.interridge.com) with seafloor hydrothermal activities and polymetallic sulfide sediments located in many different tectonic settings, including mid-ocean ridges (MOR), back-arc spreading centers, and volcanic arcs. Approximately 65% of all polymetallic sulfide sediments found are located on mid-ocean ridges. MOR sulfides are the product of ongoing hydrothermal activity and are important sulfide resources in modern seafloor hydrothermal systems (Hannington et al. 2011; Liao et al. 2019). MOR sulfides are mainly in the forms pyrite, chalcopyrite, and sphalerite, of which sphalerite is the most important host mineral for Ga. Metal (Fe, Cu, and Zn) sources of sulfides have been thoroughly investigated via their isotopes (e.g., Rouxel et al. 2004, 2008, 2018; John et al. 2008; Liu et al. 2019; Wang et al. 2020). However, the sources of Ga and the enrichment mechanisms of MOR sulfides are of great significance in understanding the global oceanic Ga cycle, which has not yet been sufficiently constrained.

Previous geophysical and geochemical studies (Georgen et al. 2001; Sauter et al. 2009; Tao et al. 2014; Jian et al. 2017; Zhu et al. 2020) have indicated that the Yuhuang and Duanqiao hydrothermal fields on the Southwest Indian Ridge (SWIR) have different hydrothermal circulation patterns and sources of metal materials, rendering them optimal objects for a study investigating the differentiation of Ga isotopes. In this article, based on a systematic study of the sulfides in these two hydrothermal fields together with the regional basalts and sediments, the sources of Ga and the mechanisms of Ga isotopic fractionation in hydrothermal systems are explored in order to establish a model of the Ga cycle in hydrothermal systems.

2. Geologic setting

The SWIR, the line that divides the Antarctic Plate from the African Plate, stretches from the Rodrigues Triple Junction (RTJ) in the east to the Bouvet Triple Junction (BTJ) in the west, and is approximately 8000 km in length (Patriat et al. 1997) (Fig. 1). It is an ultraslow-spreading MOR with a half-spreading rate of approximately 0.7–0.9 cm/yr (Dick et al. 2003). The center of this ridge contains many deep axial rifts and is cut by a series of N–S striking transform faults (Patriat et al. 1997). Topographical and geophysical surveys of the area have revealed that the characteristics of the central rift valley, including the thickness of the crust, morphology, mantle composition, and the magmatic activity along the SWIR vary significantly along the ridge axis from the BTJ to the RTJ (Georgen et al. 2001; Sauter et al. 2009; Tao et al. 2014; Jian et al. 2017). Intense hydrothermal activity has been observed along the sections lying at 49°–52°E with approximately 2.5 hydrothermal sites per 100 km, which is similar to the area lying at 36°–38°N on the Mid-Atlantic Ridge (Tao et al. 2012).

The Yuhuang hydrothermal field (49°16′E) is located between the Indomed and Gallieni transform faults on the south rift wall in Segment 29 of the SWIR (Fig. 1). This segment is characterized by typical asymmetric spreading, with a axial volcanic ridge developing in the central rift valley. The northern ridge flank contains a series of normal faults that form a graben terrain, while the southern ridge flank is composed of comparatively high land terrain (Liao et al. 2018a). The average water depth in this segment is 3180 m (Sauter, 2001). The Yuhuang hydrothermal field, which was discovered by Chinese research cruise DY-21, is located approximately 7.5 km from the ridge axis and has a relative elevation of approximately 1500 m above the floor of the central rift valley, in an area where the water is relatively shallow at 1400–1600 m (Han et al. 2010, 2015). Two sulfide accumulations with a diameter of approximately 500 m have been found in the Yuhuang hydrothermal field, and drilling data suggests the likelihood of rich

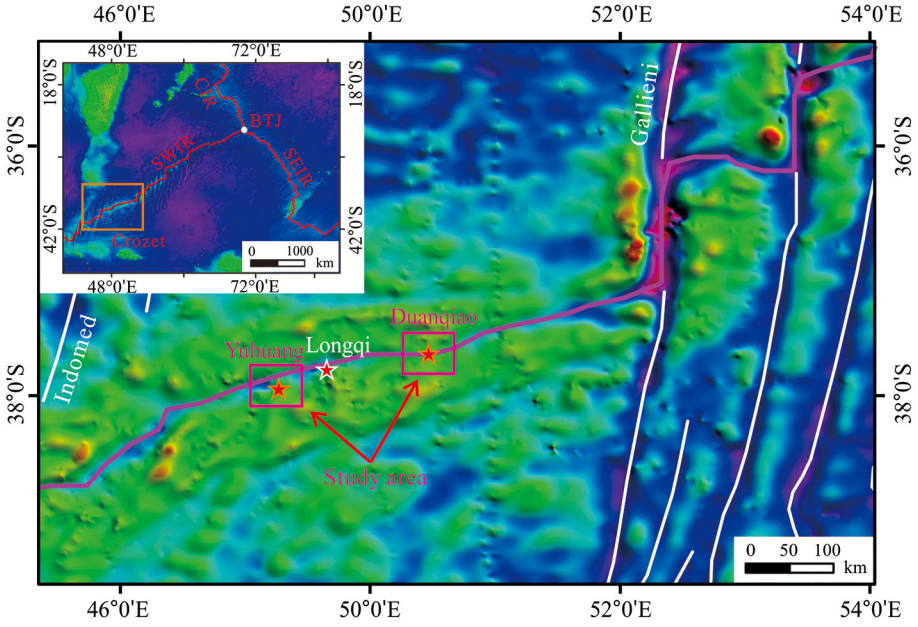

Fig. 1. Geologic map of the Southwest Indian Ridge (after Zhu et al. 2020). The ridge axis (red line) and normal faults (white lines) are inferred from the topography. Note: CIR - central Indian Ridge; SEIR - Southeast Indian Ridge; SWIR - Southwest Indian Ridge; and BTJ - Bouvet Triple Junction.

sulfides below the surface layer of calcareous sediments (Liao et al. 2018a). Based on deep tow observations, the rock surrounding the Yuhuang hydrothermal field is mainly basalt, with a small amount of ultramafic rock, suggesting the development of detachment faults (Liao et al. 2018a). The sulfides in the Yuhuang hydrothermal field are mainly composed of sphalerite and pyrite, alongside small amounts of marcasite and chalcopyrite.

The Duanqiao hydrothermal field (50°24′E) is located in the middle of Segment 27 of the SWIR, lying between the Indomed and Gallieni transform faults (Tao et al. 2012) (Fig. 1). The segment is approximately 80 km long, with the water reaching a depth of only approximately 1700 m in the middle of this segment (Cannat et al. 1999). The area is characterized by symmetric spreading, with a volcanic ridge under development on the ridge axis. Both the northern and southern flanks contain conjugate seamounts with steep slopes that face the axis and gentle slopes that face away from the axis (Mendel et al. 2003). The Duanqiao hydrothermal field was discovered during Chinese research cruise DY-20 and is located on an axial highland, surrounded by relatively flat terrane (Tao et al. 2012, 2014). The hydrothermal activity in this hydrothermal field is widespread, covering an area of approximately 200 m × 125 m (Tao et al. 2012). The sulfides in the hydrothermal field are arranged in loose accumulations or mounds, and the sulfide chimney collapse is evenly distributed. The rock surrounding the Duanqiao hydrothermal field is mainly basalt, with sulfides mainly composed of pyrite, chalcopyrite, and sphalerite.

3. Samples and methods

3.1. Samples and materials

Twenty-seven samples collected using a TV-grab system were selected for the Ga isotope analysis, including 13 sulfides, 6 basalts, and 8 calcareous sediment samples. The sulfides were mainly collected from massive sulfides, sulfide chimneys, and sulfide breccia, with eight samples from the Yuhuang hydrothermal field and five samples from the Duanqiao hydrothermal field. The basalts were collected from the MOR around the hydrothermal fields, and were unaffected by the hydrothermal activity. The calcareous samples are surface sediments, which were also unaffected by the hydrothermal activity. Each sample was cleaned with deionized water, dried, and crushed to 200 mesh (0.074 mm) prior to geochemical analyses. All acids used in this study were purified by sub-boiling distillation, and the water was 18.2 MΩ grade from a Millipore system.

3.2. Elemental analyses

A portion of each rock sample (0.1 g) was weighed into a Teflon beaker and digested using the microwave digestion technique. The Fe, Cu, Zn, Al, and Ca concentrations of the digested samples were measured using an inductively coupled plasma optical emission spectrometer (Varian Vista MPX). Concentrations were determined relative to the calibration curves. The Ga concentrations of the digested samples were measured using inductively coupled plasma-mass spectrometry (ICP-MS; PE ELAN DRC-e) and the calibration was performed using a multi-element (including Ga, Ce, La, Y, Ho, Sr, Cd, and Mo.) standard solution. The analytical uncertainty for the elemental concentrations was generally better than 5%.

For the analysis of the carbonate-phase Ga in the calcareous sediments, 0.2 g of each sample was weighed into a 50 mL centrifuge tube after which 30 mL of 1.5 M HAc solution was added. Once the strong reaction of the carbonate with the HAc subsided and stabilized, the centrifuge tubes were closed and shaken on an oscillator for at least 24 h. Subsequently, the mixture was centrifuged to separate the supernatant from the residue. The supernatant was evaporated to dryness and then dissolved in 0.15 M HNO_3 for the HAc-phase Ga (carbonate-phase Ga) concentration analysis. The residues were digested in HF and aqua regia and the Ga concentrations of the liquid samples were analyzed. The HAc-phase Ga comprises the carbonate-phase Ga proportion of total Ga (HAc-phase Ga + Ga in the residues).

3.3. Isotopic analyses

3.3.1. Ga separation

After the Ga concentrations in the powdered samples were determined, an aliquot containing more than 0.4 μg of Ga was placed in a Teflon beaker with 4 mL of concentrated HNO_3 and 4 mL of concentrated HF, and the samples were digested using microwave digestion. The sample solution was evaporated to dryness on a hot plate at 120 °C and then dissolved in 6 M HCl. The procedure described by Yuan et al. (2016), which involves the use of two chromatographic columns (loaded with AG 1-X4 and Ln-spec resin), was used to separate Ga from the matrix. This method was calibrated using both synthetic and natural samples and was validated by assessing the extraction yield (99.8% ± 0.8%, 2SD, $n = 23$) and the reproducibility (2SD uncertainty of better than 0.05‰, $n = 116$) of the measured isotopic ratio (Yuan et al. 2016). The volume of the 6 M HCl was then increased to 40 mL in order to remove as much Cu as possible from the samples, and a Cu isotope standard was added to correct the instrumental mass bias when using the MC-ICP-MS measured Ga isotopic ratios. A small amount of solution, collected from all samples before and after the chemical separation, was utilized for trace element analysis to assess the Ga recovery and the removal of the matrix. Only samples in which the Ga recovery reached 99% and potential forms of interference were negligible (Ce, La, Nd, and Fe) or correctable (Ba) were measured to determine their Ga isotopic compositions. In addition, two geological reference materials (BCR-2 and BHVO-2 basalts from the United States Geological Survey (USGS)) were prepared to monitor the chemical separation and mass spectrometry measurements.

3.3.2. Mass spectrometry measurements

The Ga isotope ratio measurements were performed on the Neptune plus multi collector ICP-MS instrument at the State Key Laboratory of Ore Deposit Geochemistry, Institute of Geochemistry, Chinese Academy of Sciences. The Ga standards and the purified samples were dissolved in 0.15 M HNO_3 for MC-ICP-MS analysis in low-resolution mode, using a Pt "Jet" sampler and a Ni "x-type" skimmer cone. A Teflon nebulizer with an uptake rate of 50 μL/min was used to introduce the sample, with Ga concentrations of the samples and standards at approximately 0.2 μg/mL. Each measurement included 50 integrations lasting 4.194 s in 5 blocks of 10 cycles. The nebulizer and spray chamber were rinsed with 0.30 M HNO_3 after each run until the signal intensity reached the original background level (generally after 4 min, $^{69}Ga < 0.5$ mV). Signal acquisition was performed using the following configurations: $^{63}Cu^+$, $^{65}Cu^+$, $^{66}Zn^+$, $^{137}Ba^{2+}$, $^{69}Ga^+$, and $^{71}Ga^+$ ion beams were collected using Faraday cups at positions L3, L1, C, H2, H3, and H4, respectively. Kato et al. (2017) reported that the interference of $^{138}Ba^{2+}$ by ^{69}Ga is significant when the Ba/Ga ratio (ppb/ppb) of a sample is $>4 \times 10^{-4}$. This interference can be corrected using $^{137}Ba^{2+}$ (with a mass of 68.5) and the equation:

$$^{69}Ga_{TRUE} = I69 - {}^{138}Ba^{2+} \approx I69 - 6.39 \times I68.5.$$

I69 represents the intensity measured with a mass of 69 and I68.5 represents the doubly ionized $^{137}Ba^{2+}$, at the mass of 68.5. The Ga isotopic ratio measurements of the Ga reference standards indicate that this calculation can correct the Ga isotopic composition of samples with Ba/Ga ratios of less than 2×10^{-2} (Kato et al., 2017). We therefore used this calculation method to correct for the interference of $^{138}Ba^{2+}$ by ^{69}Ga, as recommended by Kato et al. (2017).

Previous studies have reported that a model combining standard-sample bracketing with internal mass bias correction can produce more accurate and precise Ga isotope ratios, and that Cu is a very useful internal standard element for correcting the mass bias during Ga isotope analysis (Yuan et al. 2016; Zhang et al. 2016). Here, the ERM®-AE647 Cu solution, which was provided by the Institute for

Table 1
The $\delta^{71/69}Ga_{NIST\text{-}994}$ values of the Ga reference standards.

Reference Material	Description	$\delta^{71/69}Ga_{NIST\text{-}994}$ (‰) (2SD, $n = 8$) This Study	$\delta^{71/69}Ga_{NIST\text{-}994}$ (‰) Previous Studies
BCR-2	Basalt, from USGS	1.20 ± 0.08	+1.26* Kato et al. (2017)
BHVO-2	Basalt, from USGS	1.19 ± 0.04	+1.26* Kato et al. (2017)
Alfa Aesar Ga	Plasma standard Ga solution, lot: 8129898, supplied by Alfa Aesar China (Tianjin) Co., Ltd.	2.04 ± 0.06	
NIST 3119a Ga	Standard solution, from NIST	2.65 ± 0.04	

*$\delta^{71/69}Ga_{NIST\text{-}994}$ was re-calculated from Kato et al. (2017). The $\delta^{71/69}$Ga values of BCR-2, BHVO-2, and NIST 3119a Ga relative to the IPGP standard are −0.01‰ ± 0.01‰, −0.01‰ ± 0.05‰, and + 1.38‰ ± 0.06‰, respectively (Kato et al., 2017a). We can calculate the $\delta^{71/69}$Ga values of BCR-2 and BHVO-2 relative to NIST 3119a Ga (−1.39‰). In this study, the calculated $\delta^{71/69}$Ga values of BCR-2 and BHVO-2 relative to NIST 3119a Ga are −1.45‰ and −1.46‰, respectively, which are consistent with the measurements of Kato et al. (2017) within the applicable margin of error. To facilitate a more intuitive comparison, the $\delta^{71/69}$Ga of NIST 3119a Ga relative to NIST 994 Ga in this measurement is 2.65‰ ± 0.04‰, and we re-calculated the $\delta^{71/69}$Ga values of BCR-2 and BHVO-2 from Kato et al. (2017) relative to NIST 994 Ga, with the $\delta^{71/69}Ga_{NIST\text{-}994}$ values of both samples at +1.26‰.

Reference Materials and Measurements and has a ratio of $^{65}Cu/^{63}Cu = 0.44560 \pm 0.00074$, was employed for correction during the determination of the Ga isotope ratios. The Ga isotopic compositions are reported in the δ-notation relative to NIST SRM 994Ga, as defined by the following relationship:

$$\delta^{71/69}Ga_{NIST\text{-}994}\ (‰) = [(^{71}Ga/^{69}Ga)_{sample}/(^{71}Ga/^{69}Ga)_{NIST\text{-}994} - 1] \times 1000.$$

The $\delta^{71/69}Ga_{NIST\text{-}994}$ values of the four Ga reference standards (two geological reference materials and two Ga standard solutions), which were prepared to monitor the chemical separation and mass spectrometry measurements, are presented in Table 1.

4. Results

The $\delta^{71/69}Ga_{NIST\text{-}994}$ values and Ga, Zn, Cu, Fe, Al, and $CaCO_3$ concentrations of the samples are shown in Tables 2 and 3. The $\delta^{71/69}Ga_{NIST\text{-}994}$ values and Ga concentrations of the eight sulfide samples from the Yuhuang hydrothermal field range from +0.99‰ to +1.57‰ (with an

Table 2
The $\delta^{71/69}Ga_{NIST\text{-}994}$ values and Ga, Zn, Cu, and Fe concentrations in the samples.

Samples	Description	$\delta^{71/69}Ga_{NIST\text{-}994}$ (‰) (2SD, $n = 3$)	Ga (μg/g)	Zn (wt.%)	Cu (wt.%)	Fe (wt.%)	Al (wt.%)	$10^4 \times$ Ga/Al
	Yuhuang hydrothermal field							
SC-1	Sulfide chimney	1.57 ± 0.03	5.81	0.20	17.40	29.80	n.d.	
SC-2	Sulfide chimney	1.32 ± 0.02	4.61	0.53	4.84	16.81	n.d.	
SC-3	Sulfide chimney	1.46 ± 0.03	3.47	9.00	0.07	6.18	n.d.	
SB-1	Sulfide breccia	1.24 ± 0.02	10.41	0.15	22.61	31.11	n.d.	
SB-2	Sulfide breccia	1.00 ± 0.06	6.29	0.27	26.60	27.80	n.d.	
SB-3	Sulfide breccia	1.17 ± 0.03	9.94	0.34	8.00	24.70	n.d.	
MS-1	Massive sulfide	0.99 ± 0.06	46.02	39.61	0.62	11.82	n.d.	
MS-2	Massive sulfide	1.21 ± 0.02	2.29	1.18	0.20	11.50	n.d.	
	Average of total (8)	1.25						
	Duanqiao hydrothermal field							
MS-3	Massive sulfide	1.55 ± 0.03	1.71	0.84	6.57	23.90	n.d.	
MS-4	Massive sulfide	1.28 ± 0.02	10.71	2.37	3.87	27.21	n.d.	
MS-5	Massive sulfide	1.15 ± 0.02	4.55	0.88	2.15	27.92	n.d.	
MS-6	Massive sulfide	1.04 ± 0.03	6.78	2.43	1.07	21.01	n.d.	
MS-7	Massive sulfide	0.93 ± 0.02	29.52	2.78	0.60	17.21	n.d.	
	Average of total (5)	1.19						
BR-1	MORB	1.20 ± 0.04	17.20	71.80*	109.01*	7.12	7.73	2.23
BR-2	MORB	1.23 ± 0.02	16.21	72.71*	96.41*	7.05	7.33	2.21
BR-3	MORB	1.23 ± 0.05	18.02	73.11*	79.20*	7.18	8.30	2.17
BR-4	MORB	1.20 ± 0.04	17.00	72.30*	85.41*	7.82	7.35	2.31
BR-5	MORB	1.23 ± 0.06	15.60	71.22*	75.11*	7.23	7.02	2.22
BR-6	MORB	1.22 ± 0.02	17.51	81.21*	87.10*	7.96	7.51	2.33
	Average of total (6)	1.22						

Note: * is μg/g.

Table 3
The $\delta^{71/69}Ga_{NIST\text{-}994}$ values and major element compositions (Ga, Zn, Cu, Fe, Al, $CaCO_3$, $10^4 \times$ Ga/Al, and carbonate-phase Ga) of the sediment samples.

Samples	$\delta^{71/69}Ga_{NIST\text{-}994}$ (‰) (2SD, n = 3)	Ga (μg/g)	Zn (μg/g)	Cu (μg/g)	Fe (wt.%)	Al (wt.%)	$CaCO_3$ (wt.%)	$10^4 \times$ Ga/Al	carbonate-phase Ga (%)
SD-1	1.39 ± 0.07	1.08	11.70	18.31	0.42	0.32	91.7	3.42	0.59
SD-2	1.45 ± 0.06	2.11	26.81	24.22	1.05	0.72	80.2	2.94	0.67
SD-3	1.42 ± 0.04	1.59	20.11	25.61	0.85	0.55	82.3	2.89	0.77
SD-4	1.37 ± 0.08	1.36	13.92	30.63	0.59	0.42	79.9	3.17	0.52
SD-5	1.47 ± 0.06	2.12	21.91	50.02	0.88	0.71	73.4	2.91	0.36
SD-6	1.33 ± 0.10	0.54	7.35	6.11	0.19	0.15	88.2	3.61	0.85
SD-7	1.28 ± 0.08	0.97	16.52	12.81	0.41	0.31	82.7	3.11	0.98
SD-8	1.30 ± 0.09	0.90	19.31	7.90	0.35	0.26	83.0	3.43	0.57
Average	1.38	1.33	17.24	21.91	0.59	0.43	82.7	3.18	0.66

Note: The carbonate-phase Ga, for which the Ga in the samples was digested using 1.5 M HAc, represents the proportion of the total Ga.

average of +1.25‰) and from 2.29 μg/g to 46.02 μg/g, respectively; while the values of the five sulfide samples from the Duanqiao hydrothermal field range from +0.93‰ to +1.55‰ (with an average of +1.19‰) and from 1.71 μg/g to 29.52 μg/g, respectively. The $\delta^{71/69}Ga_{NIST\text{-}994}$ values of the six basalt samples range from +1.20‰ to +1.23‰ (with an average of +1.22‰), which are consistent with those of the two basalt standards ($\delta^{71/69}Ga_{NIST\text{-}994}$ = +1.20‰ for BCR-2 and + 1.19‰ for BHVO-2 in this study; $\delta^{71/69}Ga_{NIST\text{-}994}$ = +1.26‰ for both BCR-2 and BHVO-2 in Kato and Moynier, 2017a,b). The $\delta^{71/69}Ga_{NIST\text{-}994}$ values of the eight calcareous sediments range from +1.28‰ to +1.47‰ (with an average of +1.38‰). The Ga isotopic compositions of the calcareous sediments and basalts are both homogeneous, whereas the sulfides from the Yuhuang and Duanqiao hydrothermal fields exhibit relatively distinct Ga isotopic fractionation (of up to 0.58‰ and 0.62‰, respectively) and have a similar range of $\delta^{71/69}Ga_{NIST\text{-}994}$ values. The Fe, Zn, and Cu concentrations in the sulfides from the two hydrothermal fields are 6.18%–31.11%, 0.15%–39.61%, and 0.07%–26.60%, respectively. The concentrations of Ga, Fe, Zn, Cu, and Al in the basalt samples are 15.60–18.02 μg/g, 7.05%–7.96%, 71.22–81.21 μg/g, 75.11–109.01 μg/g, and 7.02%–8.30%, respectively. The concentrations of Ga, Fe, Zn, Cu, Al, $CaCO_3$, the carbonate-phase Ga, and the ratio of $10^4 \times$ Ga/Al in the calcareous sediments are 0.54–2.12 μg/g, 0.19%–1.05%, 7.35–26.81 μg/g, 6.11–50.02 μg/g, 0.15%–0.72%, 73.4%–91.7%, 0.36%–0.98%, and 2.89–3.61, respectively. Carbonates dominate the sediments, and the Ga, Zn, Cu, and Fe concentrations in the sediments are all relatively low.

5. Discussion

5.1. Ga occurrence in seafloor sulfides

Previous studies have suggested that Ga has three dominant forms in nature: (1) adsorbed onto the surface of minerals (Liu 1982; Wang et al. 2011), (2) in the form of independent Ga minerals (Burton and Culkin 1978; Wood and Samson 2006; Prokof'ev et al., 2016), and (3) in isomorphic substitutions (Burton and Culkin 1978; Liu 1982; Malvin and Drake 1987; Tu et al. 2003; Cook et al. 2009; Zhuang et al. 2019). We can eliminate the possibility of the adsorbed form of Ga in the sulfides because Ga is a chalcophile element, and individual Ga minerals were not found in the micro-mineral studies. Therefore, we can conclude that the dominant form of Ga in the sulfides is that of isomorphic substitution. The samples in this study are from different types of sulfide assemblages; this means that the Ga concentrations in the sulfides from the Yuhuang and Duanqiao hydrothermal fields have no correlation with the concentrations of main metal elements such as Fe, Cu, and Zn (Fig. 2). However, the form in which Ga was present in the samples could not be confirmed based on the data collected. Zhang (2019) analyzed the in-situ trace element concentrations of sphalerite, pyrite, and chalcopyrite from the Duanqiao and Longqi hydrothermal fields, with results indicating that the Ga concentrations are extremely low in pyrite and chalcopyrite, while that in sphalerite are 0.18–871.69 μg/g (Longqi hydrothermal field) and 0.03–460.55 μg/g (Duanqiao hydrothermal field). Thus, the Ga is mainly present within sphalerite. In-situ analyses of the sphalerite have shown that Ga is present within the lattice of sphalerites in the dominant form of substitution ($2Zn^{2+} \leftrightarrow Cu^{+} + Ga^{3+}$) (Cook et al. 2009; Zhang, 2019; Zhuang et al. 2019). We also conclude that, of the sulfides analyzed in this study, Ga occurs mainly in sphalerite.

5.2. Ga isotopic compositions in basalts and sediments

The results of this study indicate Ga concentrations of 15.60–18.02 μg/g in the MORB samples, which is slightly higher than the Ga concentrations (13.0–16.0 μg/g) in MORBs reported by Kato et al. (2017). Although the Ga concentration is not uniform within the MORBs, the range of the $\delta^{71/69}Ga_{NIST\text{-}994}$ values in the six MORB samples is very narrow (+1.20‰ to +1.23‰, with an average of +1.22‰) in this study, which is consistent with the $\delta^{71/69}Ga_{NIST\text{-}994}$ values of the two basalt standards (BCR-2 and BHVO-2) within the applicable margin of error, and is also consistent with the $\delta^{71/69}Ga_{NIST\text{-}994}$ values for MORBs reported by Kato et al. (2017) (Fig. 3). This suggests that, despite the heterogeneous Ga concentration in the MORBs, the isotopic composition is homogeneous, and therefore the Ga isotopes may either not fractionate at all or only slightly fractionate under high-temperature geological processes.

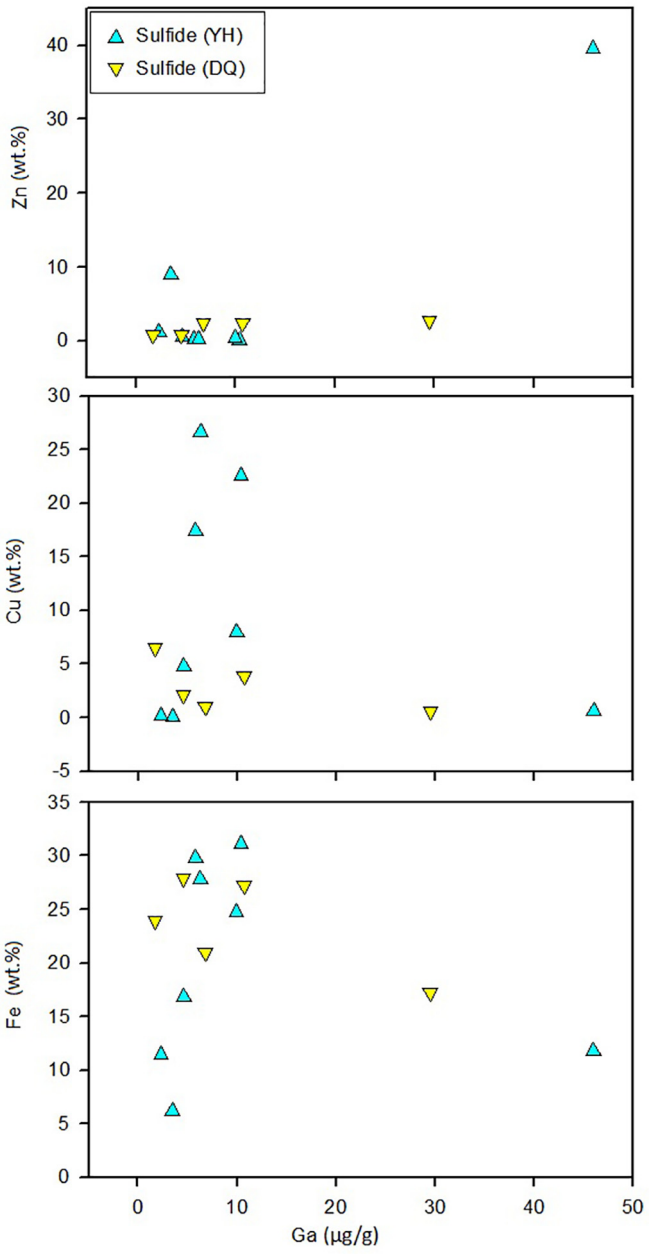

Fig. 2. Plots of Ga vs. Zn, Cu, and Fe for the sulfides from the Yuhuang and Duanqiao hydrothermal fields. YH - Yuhuang hydrothermal field; DQ - Duanqiao hydrothermal field.

The Ga isotopic compositions of seafloor sediments have not been previously reported. Despite the fact that the Ga concentrations in the sediments vary significantly (0.54–2.12 μg/g), the range of the $\delta^{71/69}Ga_{NIST\text{-}994}$ values within the sediments are narrow (+1.28‰ to +1.47‰, average of +1.38‰), which implies that Ga isotopes may fractionate slightly during the formation of sediments. Overall, compared to the basalts ($\delta^{71/69}Ga_{NIST\text{-}994}$ values of +1.20‰ to +1.23‰), the sediments ($\delta^{71/69}Ga_{NIST\text{-}994}$ values of +1.28‰ to +1.47‰) are richer in

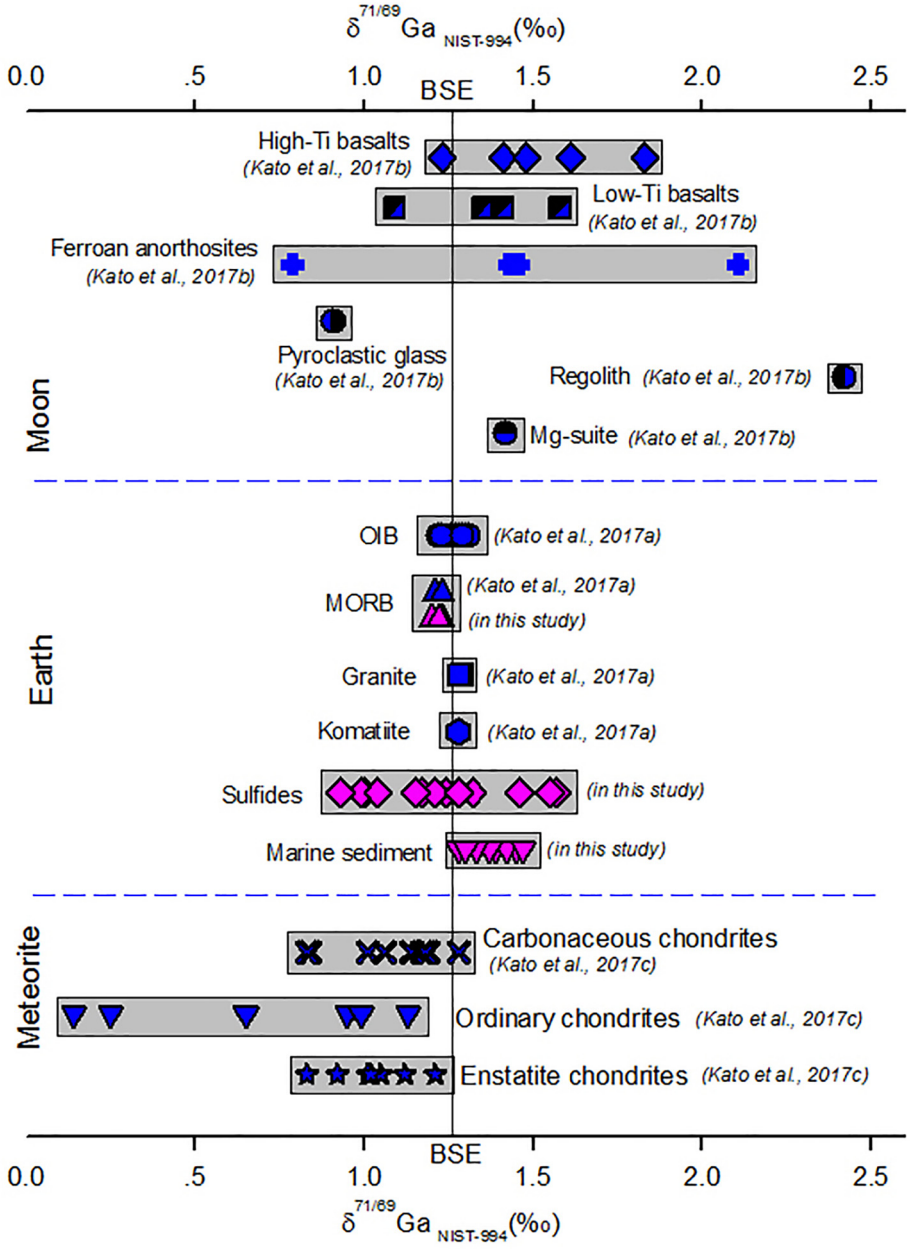

Fig. 3. Comparison of the Ga isotopic compositions obtained in this study with those from the literature.

heavier Ga isotopes (Fig. 3). Detailed reports on the sources of Ga in sediments have not been published. Carbonates were predominant in the sediments analyzed in this study (with $CaCO_3$ concentrations of 73.4%–91.7%), whereas the concentration of the carbonate-phase Ga in all the calcareous sediments was lower than 1% (Table 3). This implies that the theory suggesting that Ga is adsorbed by the carbonate or dissolved in the pore water can be neglected. Previous studies have suggested that basaltic debris and (Mn, Fe) hydroxides are also important components of the surface sediments in Southwest Indian Ocean MOR regions (Liao et al. 2018b). The $\delta^{71/69}Ga_{NIST\text{-}994}$ values and Ga/Al ratios of the basalts are both relatively homogeneous. However, the range of the $\delta^{71/69}Ga_{NIST\text{-}994}$ values in the sediments differ from that of the basalts while the range of Ga/Al ratios are wider than those of the basalts (Fig. 4), and the concentrations of Ga and Fe in the sediments exhibit a significant positive correlation (Fig. 5a). This suggests that basaltic debris makes a minor contribution to the Ga in the sediments, and the

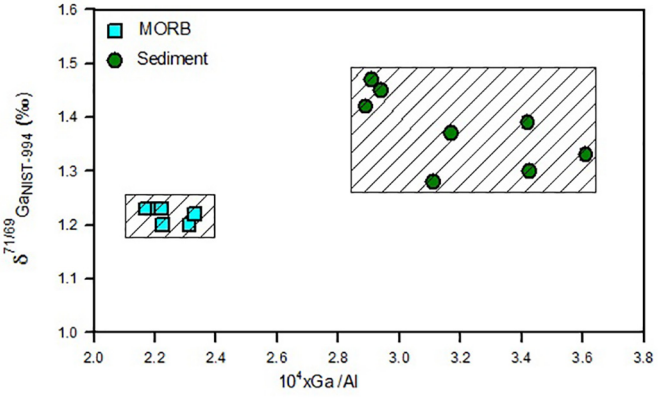

Fig. 4. Plot of $\delta^{71/69}Ga_{NIST\text{-}994}$ vs. $10^4 \times$ Ga/Al for sediments and basalts.

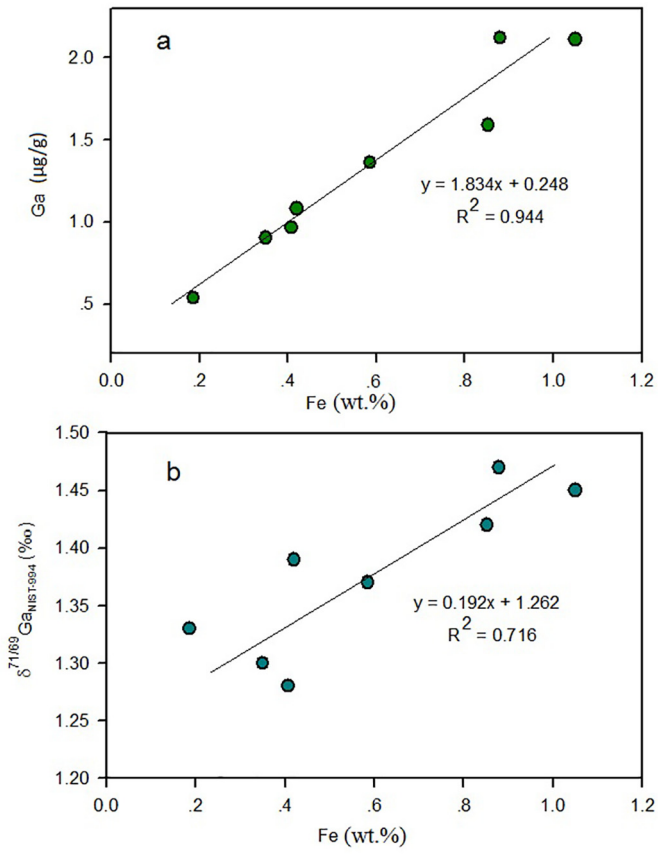

Fig. 5. Plots of Fe concentrations vs. Ga concentrations and $\delta^{71/69}Ga_{NIST\text{-}994}$ in sediments.

Ga in the sediments mainly originates from the (Fe, Mn) oxides. Yuan et al. (2018) concluded that goethite can adsorb Ga in solution when the pH is 2.5–10.5. This suggests that both goethite and the Ga adsorbed by it are insoluble in weak acids, suggesting that in this study the 1.5 M HAc digested both the carbonate and the Ga within it, whereas it did not digest the Ga in the Fe oxides/hydroxides. In Fig. 5, the Ga concentrations and $\delta^{71/69}Ga_{NIST\text{-}994}$ values of the sediments both have good positive correlations with the Fe concentrations. This implies that the Ga in the sediments may have mainly originated from the soluble Ga in the seawater, which was adsorbed by the Fe oxides/hydroxides. Based on the study by Yuan et al. (2018), equilibrium fractionation of Ga isotopes occurs when goethite adsorbs the Ga in the water, with the $\Delta^{71}Ga_{solid\text{-}solution}$ ranging from −0.45‰ to −0.89‰. Assuming that the Ga isotope fractionation between sediments and seawater has achieved an equilibrium in modern oceans, we speculate that the $\delta^{71/69}Ga_{NIST\text{-}994}$ value of the seawater in the study area is within the range from +1.92‰ to +2.36‰.

5.3. Ga isotopic compositions of the sulfides

The $\delta^{71/69}Ga_{NIST\text{-}994}$ values of the sulfides from the Yuhuang hydrothermal field range from +0.99‰ to +1.57‰ (average of +1.25‰), while the $\delta^{71/69}Ga_{NIST\text{-}994}$ values of the sulfides from the Duanqiao hydrothermal field range from +0.93‰ to +1.55‰ (average of +1.19‰) (Table 2). The ranges of the $\delta^{71/69}Ga_{NIST\text{-}994}$ values of the sulfides from the two hydrothermal fields are similar, and the average $\delta^{71/69}Ga_{NIST\text{-}994}$ values of the sulfides are close to that of the MORB (Table 2 and Fig. 6). Previous studies have shown that the Yuhuang area is a detachment fault-type hydrothermal field (Liao et al. 2018a); while the Duanqiao area is a magmatic-controlled hydrothermal field. Based on geophysical data, an axial magma chamber is present 9 km below the seafloor (Sauter et al. 2009; Li et al. 2015; Jian et al. 2017; Sun et al. 2018). A recent study suggests that the metals in the Yuhuang hydrothermal field are derived from both seawater and magmatites, while the metals in the Duanqiao hydrothermal field are derived only from magmatites (Zhu et al. 2020). As the study area is a sediment-free MOR and sediments are extremely rare, the sediments are usually considered to contribute less to the metals in these types of hydrothermal fields. Thus, the Ga in the Yuhuang hydrothermal field may have been derived from a mixture of seawater and magmatites, while the Ga in the Duanqiao hydrothermal field may have been derived solely from magmatites. The mean $\delta^{71/69}Ga_{NIST\text{-}994}$ values of the sulfides in the Yuhuang and Duanqiao hydrothermal fields are 1.25‰ and 1.19‰, respectively, which is consistent with that of the basalts. This implies that the Ga in the two hydrothermal fields has the same source, in that it mainly originates from the basalts. Based on existing models, the volume ratio of the water–rock reactions is approximately from 1 to 4 in sulfide hydrothermal fields (Gregory and Taylor 1981). Moreover, the Ga concentrations of seawater are 2–56 pmol/kg (Orians and Bruland 1988; Shiller 1998; Shiller and Bairamadgi 2006; McAlister and Orians 2015), and the Ga concentrations of basalts are approximately 4×10^6 to 1×10^8 times that of seawater. Therefore, we speculate that no or very little of the Ga in the sulfides was derived from seawater. In conclusion, the Ga in the sulfides in the Yuhuang and Duanqiao hydrothermal regions mainly originated from the leaching of MORB.

Ga isotopic behavior in hydrothermal systems is still unknown. We could infer that some geological processes (such as fluid–seawater mixing, magmatic processes, and sulfide precipitation) may contribute to the Ga isotope fractionation occurring in hydrothermal systems. According to the previous discussion, the contribution of seawater to Ga in sulfides is very small, and it is probably derived from the Ga leaching of MORB. The Ga isotopic compositions in MORB are homogeneous. Therefore, we infer that fluid–seawater mixing and magmatic processes have little effect on the Ga isotope fractionation in sulfides. To sum up, the samples analyzed in this study indicate that the Ga isotopic fractionation in hydrothermal systems can reach 0.64‰, which may be mainly related to the rapid precipitation during the formation of sulfides and the admixing of the different stages of sulfide. Further Ga isotope investigation would be helpful to understand the processes that lead to Ga isotope fractionation in hydrothermal systems.

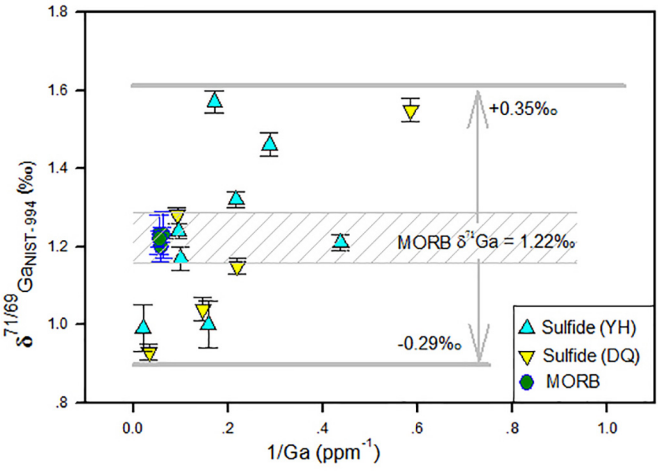

Fig. 6. Correlation between the Ga concentrations and isotopic compositions of the Yuhuang and Duanqiao hydrothermal fields. YH - Yuhuang hydrothermal field; DQ - Duanqiao hydrothermal field.

6. Conclusions

(i) The $\delta^{71/69}Ga_{NIST\text{-}994}$ values of the basalts from the SWIR range from +1.20‰ to +1.23‰, with an average of +1.22‰, which are consistent with the values of the two basalt standard samples (BCR-2 and BHVO-2), within the applicable margin of error. The $\delta^{71/69}Ga_{NIST\text{-}994}$ values of the sulfides from the Yuhuang hydrothermal field range from +0.99‰ to +1.57‰ (+1.25‰ on average), and the $\delta^{71/69}Ga_{NIST\text{-}994}$ values of the sulfides from the Duanqiao hydrothermal field range from +0.93‰ to +1.55‰ (+1.19‰ on average). The ranges of the $\delta^{71/69}Ga_{NIST\text{-}994}$ values in the sulfides from the two hydrothermal fields are almost the same, and their mean $\delta^{71/69}Ga_{NIST\text{-}994}$ values are very close to those of mid-oceanic ridge basalts.

(ii) Ga in the sulfides from the Yuhuang and Duanqiao hydrothermal fields mainly originates from MORBs. The Ga isotopic fractionation in the sulfides reaches 0.64‰, which may be mainly related to processes that lead to the formation of sulfides.

(iii) Ga in the sediments mainly originates from the soluble Ga in seawater adsorbed by Fe oxides/hydroxides. The $\delta^{71/69}Ga_{NIST\text{-}994}$ value of seawater in the study area is within the range from +1.92‰ to +2.36‰.

Declaration of Competing Interest

The authors declare that they have no known competing financial interests or personal relationships that could have appeared to influence the work reported in this paper.

Acknowledgments

This work was financially supported by the National Key R&D Program of China (Grant No. 2017YFC0602503), the National Natural Science Foundation of China (Grant Nos. 41890841, 42006074 and 41573007), China Ocean Mineral Resources R & D Association Project (DY135-S1-1-02), and a special fund managed by the State Key Laboratory of Ore Deposit Geochemistry. We thank Professor Sheng-Ao Liu and another anonymous reviewer for their very useful and constructive comments to the initial version of this work. We also thank the Associate Editor Dr. Christopher Spencer, and Dr. Lily Wang for their handling of the manuscript and editorial input.

References

Zhang, B.S., 2019. Study of mineralization at the Longqi and Duanqiao hydrothermal fields, Southwest Indian Ridge. Ph.D. thesis. China University of Geosciences (Beijing) 238 pp (in Chinese with English abstract).

Burton, J.D., Culkin, F., 1978. Gallium. In: Wedepohl, K.H. (Ed.), Handbook of Geochemistry II-3. Springer-Verlag, Berlin 32-D-7.

Cannat, M., Rommevaux-Jestin, C., Sauter, D., Deplus, C., Mendel, V., 1999. Formation of the axial relief at the very slow spreading Southwest Indian Ridge (49° to 69°E). J. Geophys. Res. Atmos. 104 (B10), 22825–22843.

Cook, N.J., Ciobanu, C.L., Pring, A., Skinner, W., Shimizu, M., Danyushevsky, L., Saini-Eidukat, B., Melcher, F., 2009. Trace and minor elements in sphalerite: a LA-ICPMS study. Geochim. Cosmochim. Acta. 73, 4761–4791.

Corliss, J.B., Dymond, J., Gordon, L.I., Edmond, J.M., Von Herzen, R.P., Ballard, R.D., Green, K., Williams, D., Bainbridge, A., Crane, K., van Andel, T.H., 1979. Submarine thermal springs on the Galápagos Rift. Science 203, 1073–1083.

De Laeter, J.R., 1972. The isotopic composition and elemental abundance of gallium in meteorites and in terrestrial samples. Geochim. Cosmochim. Acta. 36, 735–743.

Dick, H.J., Lin, J., Schouten, H., 2003. An ultraslow-spreading class of ocean ridge. Nature 426 (6965), 405–412.

Fleischer, M., 1955. Minor elements in some sulfide minerals. Econ. Geol. 970-1024.

Georgen, J.E., Lin, J., Dick, H.J.B., 2001. Evidence from gravity anomalies for interactions of the Marion and Bouvet hotspots with the Southwest Indian Ridge: Effects of transform offsets. Earth Planet. Sci. Lett. 187 (3–4), 283–300.

Gregory, R.T., Taylor, H.P., 1981. An Oxygen Isotope Profile in a section of cretaceous Oceanic Crust, Samail Ophiolite, Oman: evidence for $\delta^{18}O$ Buffering of the Oceans by deep (>5 km) Seawater-Hydrothermal Circulation at Mid-Ocean Ridges. J. Geophys. Res. 86, 2737–2755.

Han, X.Q., Wu, G.H., Cui, R., Qiu, Z.Y., Deng, X.M., Wang, Y., Dy, S.P.O., Leg, C., 2010. Discovery of a Hydrothermal Sulfide Deposit on the Southwest Indian Ridge at 49.2°E. American Geophysical Union (Fall Meeting, abstract#S21C-S1531C).

Han, X.Q., Wang, Y.J., Qiu, Z.Y., Liu, Y., Qiu, B.B., 2015. Discovery and mineralization features of the Yuhuang-1 hydrothermal field on Southwest Indian Ridge. Acta Mineral. Sin. 35 (S1), 1141–1142 (in Chinese with English abstract).

Hannington, M., Jamieson, J., Monecke, T., Petersen, S., Beaulieu, S., 2011. The abundance of seafloor massive sulfide deposits. Geology 39 (12), 1155–1158.

Inghram, M.G., Hess, D.C.J., 1948. On the isotopic composition of meteoritic and terrestrial Gallium. Phys. Rev. 74, 343–344.

Jian, H.C., Chen, Y.J., Singh, S.C., Li, J.B., Zhao, M.H., Ruan, A.G., Qiu, X.L., 2017. Seismic structure and magmatic construction of crust at the ultraslow-spreading Southwest Indian Ridge at 50°28′E. J. Geophys. Res. Solid Earth 122 (1), 18–42.

John, S.G., Rouxel, O.J., Craddock, P.R., Engwall, A.M., Boyle, E.A., 2008. Zinc stable isotopes in seafloor hydrothermal vent fluids and chimneys. Earth Planet. Sci. Lett. 269, 17–28.

Kato, C., Moynier, F., 2017a. Gallium isotopic evidence for extensive volatile loss from the Moon during its formation. Science Advances 3, e1700571. https://doi.org/10.1126/sciadv.1700571.

Kato, C., Moynier, F., 2017b. Gallium isotopic evidence for the fate of moderately volatile elements in planetary bodies and refractory inclusions. Earth Planet. Sci. Lett. 479, 330–339.

Kato, C., Moynier, F., Foriel, J., Teng, F.Z., Puchtel, I.S., 2017. The gallium isotopic composition of the bulk silicate Earth. Chem. Geol. 448, 164–172.

Li, J.B., Jian, H.C., Chen, Y.J., Singh, S.C., Ruan, A., Qiu, X.L., Zhao, M.H., Wang, X.G., Niu, X.W., Ni, J.Y., Zhang, J.Z., 2015. Seismic observation of an extremely magmatic accretion at the ultraslow spreading Southwest Indian Ridge. Geophysical Research Letters 42 (8), 2656–2663.

Liao, S.L., Tao, C.H., Li, H.M., Barriga, F.J.A.S., Liang, J., Yang, W.F., Yu, J.Y., Zhu, C.W., 2018a. Bulk geochemistry, sulfur isotope characteristics of the Yuhuang-1 hydrothermal field on the ultraslow-spreading Southwest Indian Ridge. Ore Geol. Rev. 96, 13–27.

Liao, S.L., Tao, C.H., Li, H.M., Zhang, G.Y., Liang, J., Yang, W.F., Wang, Y., 2018b. Surface sediment geochemistry and hydrothermal activity indicators in the Dragon Horn area on the Southwest Indian Ridge. Mar. Geol. 398, 22–34.

Liao, S.L., Tao, C.H., Zhu, C.W., Li, H.M., Li, X.H., Liang, J., Yang, W.F., Wang, Y.J., 2019. Two episodes of sulfide mineralization at the Yuhuang-1 hydrothermal field on the Southwest Indian Ridge: Insight from Zn isotopes. Chem. Geol. 507, 54–63.

Liu, Y.J., 1982. Chief genetical types of Gallium-Bearing deposits in China. Mineral Deposits 1, 51–60 (in Chinese with English abstract).

Liu, S.A., Liu, P.P., Lv, Y.W., Wang, Z.Z., Dai, J.G., 2019. Cu and Zn isotope fractionation during oceanic alteration: Implications for Oceanic Cu and Zn cycles. Geochim. Cosmochim. Acta. 257, 191–205.

Malvin, D.J., Drake, M.J., 1987. Experimental determination of crystal/melt partitioning of Ga and Ge in the system forsterite-anorthite-diopside. Geochim. Cosmochim. Acta. 51 (8), 2117–2128.

McAlister, J.A., Orians, K.J., 2015. Dissolved gallium in the Beaufort Sea of the Western Arctic Ocean: a GEOTRACES cruise in the International Polar Year. Mar. Chem. 177, 101–109.

Meija, J., Coplen, T.B., Berglund, M., Brand, W.A., De Bièvre, P., Gröning, M., Holden, N.E., Irrgeher, J., Loss, R.D., Walczyk, T., Prohaska, T., 2016. Isotopic compositions of the elements 2013 (IUPAC technical report). Pure Appl. Chem. 88, 293–306.

Mendel, V., Sauter, D., Rommevaux-Jestin, C., Patriat, P., Lefebvre, F., Parson, L.M., 2003. Magmato-tectonic cyclicity at the ultra-slow spreading Southwest Indian Ridge: evidence from variations of axial volcanic ridge morphology and abyssal hills pattern. Geochem. Geophys. Geosyst. 4 (5), 9102. https://doi.org/10.1029/2002GC000417.

Moskalyk, R.R., 2003. Gallium: the backbone of the electronics industry. Miner. Eng. 16, 921–929.

Orians, K.J., Bruland, K.W., 1988. Dissolved gallium in the open ocean. Nature 332, 717–719.

Patriat, P., Sauter, D., Munschy, M., Parson, L., 1997. A survey of the Southwest Indian Ridge Axis between Atlantis II Fracture Zone and the Indian Ocean Triple Junction: Regional setting and large Scale Segmentation. Mar. Geophys. Res. 19, 457–480.

Prokof'ev, V.Y., Naumov, V.B., Dorofeeva, V.A., 2016. Gallium Concentration in Natural Melts and Fluids. Geochem. Int. 54 (8), 691–705. https://doi.org/10.1134/S0016702916080097.

Rouxel, O., Fouquet, Y., Ludden, J.N., 2004. Copper Isotope systematics of the lucky strike, Rainbow, and Logatchev Sea-floor hydrothermal fields on the mid-Atlantic Ridge. Econ. Geol. 99, 585–600.

Rouxel, O., Shanks, III, Bach, W., Edwards, K.J., 2008. Integrated Fe- and S-isotope study of seafloor hydrothermal vents at East Pacific rise 9-10°N. Chem. Geol. 252, 214–227.

Rouxel, O., Toner, B., German, Y., Glazer, B., 2018. Geochemical and iron isotopic insights into hydrothermal iron oxyhydroxide deposit formation at Loihi Seamount. Geochim. Cosmochim. Acta. 220, 449–482.

Sauter, D., Patriat, P., Rommevaux-Jestin, C., Cannat, M., Briais, A., 2001. The Southwest Indian Ridge between 49°15′E and 57°E: Focused accretion and magma redistribution. Earth Planet. Sci. Lett. 192 (3), 303–317.

Sauter, D., Cannat, M., Meyzen, C., Bezos, A., Patriat, P., Humler, E., Debayle, E., 2009. Propagation of a melting anomaly along the ultraslow Southwest Indian Ridge between 46°E and 52°20′E: interaction with the Crozet hotspot? Geophys. J. Int. 179 (2), 687–699.

Shiller, A.M., 1998. Dissolved gallium in the Atlantic Ocean. Mar. Chem. 61, 87–99.

Shiller, A.M., Bairamadgi, G.R., 2006. Dissolved gallium in the northwest Pacific and the south and central Atlantic Oceans: Implications for aeolian Fe input and a reconsideration of profiles. Geochem. Geophys. Geosyst 7, Q08M09. https://doi.org/10.1029/2005GC001118.

Sun, C.F., Wu, Z.C., Tao, C.H., Ruan, A.G., Zhang, G.Y., Guo, Z.K., Huang, E.X., 2018. The deep structure of the Duanqiao hydrothermal field at the Southwest Indian Ridge. Acta Oceanol. Sin. 37 (3), 73–79.

Tao, C.H., Lin, J., Guo, S.Q., John Chen, Y.S., Wu, G.H., Han, X.Q., German, C.R., Yoerger, D.R., Zhou, N., Li, H.M., Su, X., Zhu, J., 2012. First active hydrothermal vents on an ultraslow-spreading center: Southwest Indian Ridge. Geology 40 (1), 47–50.

Tao, C.H., Li, H.M., Jin, X.B., Zhou, J.P., Wu, T., He, Y.H., Deng, X.M., Gu, C.H., Zhang, G.Y., Liu, W.Y., 2014. Seafloor hydrothermal activity and polymetallic sulfide exploration on the southwest Indian ridge. Chin. Sci. Bull. 59, 2266–2276. https://doi.org/10.1007/s11434-014-0182-0.

Tu, G.Z., Gao, Z.M., Hu, R.Z., Zhang, Q., Li, C.Y., Zhao, Z.H., Zhang, B.G., 2003. The Geochemistry and Ore-Forming Mechanism of the Dispersed Elements. Geological Publishing House, Beijing, pp. 368–395 (in Chinese).

Wang, W.F., Qin, Y., Liu, X.H., Zhao, J.L., Wang, J.Y., Wu, G.D., Liu, J.T., 2011. Distribution, occurrence and enrichment causes of gallium in coals from the Jungar Coalfield, Inner Mongolia. Sci. China Earth Sci. 54 (7), 1053–1068. https://doi.org/10.1007/s11430-010-4147-0.

Wang, S.J., Sun, W.D., Huang, J., Zhai, S.K., Li, H.M., 2020. Coupled Fe–S isotope composition of sulfide chimneys dominated by temperature heterogeneity in seafloor hydrothermal systems. Sci. Bull. 65 (20), 1767–1774. https://doi.org/10.1016/j.scib.2020.06.017.

Williams, D.L., Green, K., Van Andel, T.H., Von Herzen, R.P., Dymond, J.R., Crane, K., 1979. Hydrothermal mounds of the Galapagos Rift: Observations with DSRV Alvin and detailed heat flow studies. J. Geophys. Res. 84, 7467–7484.

Wood, S.A., Samson, I.M., 2006. The aqueous geochemistry of gallium, germanium, indium and scandium. Ore Geol. Rev. 28, 57–102.

Yuan, W., Chen, J.B., Birck, J.L., Yin, Z.Y., Yuan, S.L., Cai, H.M., Wang, Z.W., Huang, Q., Wang, Z.H., 2016. Precise analysis of Gallium isotopic composition by MC-ICP-MS. Anal. Chem. 88, 9606–9613. https://doi.org/10.1021/acs.analchem.6b02317.

Yuan, W., Saldi, G.D., Chen, J.B., Zuccolini, M.V., Birck, J.-L., Liu, Y.J., Schott, J., 2018. Gallium isotope fractionation during Ga adsorption on calcite and goethite. Geochim. Cosmochim. Acta. 223, 350–363.

Zhang, T., Zhou, L., Yang, L., Wang, Q., Feng, L.P., Liu, Y.S., 2016. High precision measurements of gallium isotopic compositions in geological materials by MC-ICP-MS. J. Anal. At. Spectrom. 31, 1673–1679.

Zhu, C.W., Tao, C.H., Yin, R.S., Liao, S.L., Yang, W.F., Liu, J., Barriga, F.J.A.S., 2020. Seawater versus mantle sources of mercury in sulfide-rich seafloor hydrothermal systems, Southwest Indian Ridge. Geochim. Cosmochim. Acta. 281, 91–101.

Zhuang, L.L., Song, Y.C., Liu, Y.C., Fard, M., Hou, Z.Q., 2019. Major and trace elements and sulfur isotopes in two stages of sphalerite from the world-class Angouran Zn–Pb deposit, Iran: Implications for mineralization conditions and type. Ore. Geol. Rev. 109, 184–200.